NJC

Accepted Manuscript

This is an *Accepted Manuscript*, which has been through the Royal Society of Chemistry peer review process and has been accepted for publication.

Accepted Manuscripts are published online shortly after acceptance, before technical editing, formatting and proof reading. Using this free service, authors can make their results available to the community, in citable form, before we publish the edited article. We will replace this *Accepted Manuscript* with the edited and formatted *Advance Article* as soon as it is available.

You can find more information about *Accepted Manuscripts* in the **Information for Authors**.

Please note that technical editing may introduce minor changes to the text and/or graphics, which may alter content. The journal's standard **Terms & Conditions** and the **Ethical guidelines** still apply. In no event shall the Royal Society of Chemistry be held responsible for any errors or omissions in this *Accepted Manuscript* or any consequences arising from the use of any information it contains.

www.rsc.org/njc

Computational Thermodynamic Study on the Complexes of Am(III) with Tridentate N-donor Ligands

Yan-Ni Liang[ab], Xia Yang,[c] Songdong Ding,[b] Shoujian Li,[b] Fan Wang,[*b] Zhifang Chai[cd] and Dongqi Wang [*c]

[a]Shaanxi Collaborative Innovation Center of Chinese Medicinal Resources Industrialization, Shaanxi University of Chinese Medicine, Xianyang, 712046

[b]Institute of Atomic and Molecular Physics, College of Chemistry, Sichuan University, Chengdu, 610065

[c]Multidisciplinary Initiative Center, Institute of High Energy Physics, Chinese Academy of Sciences, Beijing, 100049

[d]School of Radiation Medicine and Interdisciplinary Sciences (RAD-X), Soochow University, Suzhou, 215123, China

[a]SNTCM, Xianyang
[b] Sichuan Univ., Chengdu
[c] IHEP, Beijing
[d] RAD-X, Soochow Univ., Suzhou

Corresponding Author

*E-mail: dwang@ihep.ac.cn (D.Wang), wangf44@gmail.com (F.Wang)

Abstract

To assess the role of the lateral triazine group of 2,6-bis(1,2,4-triazin-3-yl) pyridine (BTP) when coordinated to Am(III), three tridentate N-donor ligands, i.e. BTP, 6-(-2-pyridyl)-2-pyridyl (hemi-BTP), and 2,2':6'2''-terpyridine (TPY), have been used to construct coordination complexes with Am(III), and the structures and bonding modes of these complexes have been investigated using B3LYP functional. The 1:1 and 1:2 (metal:ligand) type complexes, based our calculations, form mainly via reactions of $Am(H_2O)_3(NO_3)_3 + L \rightarrow AmL(NO_3)_3 + 3H_2O$ and $[Am(H_2O)_6(NO_3)_2]^+ + 2L \rightarrow [AmL_2(NO_3)_2]^+ + 6H_2O$. The Gibbs free energy changes were in the order TPY > hemi-BTP > BTP, independent of the presence of nitrate ions in the complexes. We show that in 1:1 type complexes substitution of electron-donating groups to the three ligands can enhance their binding ability. From analysis of NPA charge and Mayer Bond Order, it is found that the value of binding free energy is correlated with the charge transfers between the central metal and the ligand: the larger the ligand-to-metal charges transfer, the more negative the binding energy, and meanwhile, the smaller the Mayer bond order of the Am-N bonds. This suggests that the interaction between Am(III) and the tridentate ligands has strong ionic feature, which is confirmed by the quantum theory of atoms-in-molecules (QTAIM) topological analysis. According to our calculations, the presence of triazine group in BTP and hemi-BTP does not improve the binding affinity of the ligand to Am(III), compared to TPY, but does facilitate the the ligand to adopt a conformation that favors to coordinate with Am^{3+} than the others via a dynamic isomerization process, and the electron-donating groups on triazine group may enhance the charge transfer between Am(III) and the ligand, and thus stabilize the complex. We tentatively propose that the facile conversion between the conformations of BTP, which is more difficult for TPY and hemi-BTP, may significantly contribute to its higher affinity towards the binding with Am(III).

1. Introduction

The separation of trivalent actinide (An) from lanthanide (Ln) cations currently mainly adopts liquid-liquid extraction protocols.[1-3] The performance of a good extractant is determined by its efficiency and selectivity toward actinides, its ability to survive from hydrolysis and radiolysis in acidic media, and ideally composed of only C, H, O, N atoms to avoid the generation of solid waste during incineration.[4, 5] The bistriazinyl-pyridine (BTP) family has been reported to be promising for An(III)/Ln(III) separation.[6, 7] With high structural similarity with BTPs, the 6-(1,2,4-triazin-3-yl)-2,2'-bipyridine ligands (hemi-BTPs)[8] were also studied and shown to be have in a way between the BTPs and the 2,2':6',2"-terpyridine ligands (TPYs).[9-11] Hemi-BTP is more analogous to TPY in its extraction behavior occuring only at low acidity and a synergist is required, and only 1:1 complexes are formed, which is different from the more hydrophobic 1:3 complexes formed by the BTPs.[9-12] Earlier experiments show that[8, 12, 13] in the absence of a lipophilic anion, e.g. 2-bromodecanoic acid, as a synergist in the organic phase, both hemi-BTP and hemi-BTBP were unable to extract Am(III) or Eu(III) from nitric acid solutions into organic phase (usually n-octanol), which is in sharp contrast to those bis-triazine ligands such as BTP and BTBP. These results demonstrate that replacement of one of the two 1,2,4-triazine rings in the BTP and BTBP ligands by a pyridine ring may inhibit their extraction performance, and emphasize the importance of the two 1,2,4-triazine rings in order to obtain optimum performance. In addition, by comparing the selectivity of tridentate ligands and bidentate ligands, Hudson et al. concluded that the central pyridine has a great contribution to the favorable extraction properties of the BTPs,[13] even if the bonding mode of the complexes of actinide with N-donor ligand remains unclear.

Most of the previous computational studies focused on the application of quantum chemistry to assess the extent of covalency in the An-N and Ln-N bonds. In these studies, quantum-chemical analysis tools, e.g. Natural Population Analysis (NPA) and Bond Overlap Populations were used to analyze the nature of the metal-ligand bond, while by far there is no consensus conclusion implicated by these calculations. Ab initio calculations were performed by Ionova et al.[14] to provide insight into the factors that govern the complexation mechanism of Ln^{3+} and planar tridentate N-ligands, in which the stability of complexes $[LnL]^{3+}$ was shown to increase with the electron donor ability of the coordinating central nitrogen atom (N_c) of the ligand and the electron acceptor ability of the coordinating lateral ones (N_l). The $[EuL]^{3+}$ complex stability increases from BTP to TPY along with the covalent parameter OP for Eu-N_l bonds but slightly decreases for Eu-N_c bonds. The difference in the effective charges on the

lateral and central nitrogen atoms are the main factors governing the formation of complexes between trivalent lanthanides and planar tridentate N-ligands. Guillaumont[15] used density functional theory (DFT)[16] to study TPY and 2,6-bis(5,6-dimethy-1,24-triazin-3-yl) pyridine (MeBTP) complexes of a range of lanthanides and actinides. The study indicated there is no significant $5f$ contribution of americium (Am) and curium (Cm) to the bonding while the participation of the metal $5f$ orbitals is significant in the uranium-ligand bond. The metal-ligand bond in this work (La, Ce, Nd, U, Pu, Am and Cm) is predominantly ionic. Covalency is present through ligand-to-metal electron donation and slightly more pronounced for actinides than for lanthanides. In the BP86 study of $[M(BTP)_3]^{3+}$ by Petit et al.,[17] the donation of f (Cm) orbitals appears to be a key factor in Cm(III) selective complexation with BTP and the covalency is larger within the Cm-BTP bond than the Gd equivalent. The Conductor-like Screening Model of solvation (COSMO)[18-20] was adopted to take into account of electrostatic effects. The study of 1:1 complexation of trivalent actinides and lanthanides with 2-amino-4,6-di-(pyridin-2-yl)-1,3,5-triazine (ADPTZ)[21] reported a mainly ionic feature for the An^{3+}/Ln^{3+}-L bonding with minor covalency, and a comparison of BTBPs complexes[22] indicated that the presence of substituents with strong electron-donating ability may strengthen the gas-phase binding stabilities.

The current study aims at understanding the complexation of BTPs, hemi-BTPs and TPYs with trivalent actinide, including the role of the lateral triazine ring, and the substitution effect of the lateral rings. A schematic elucidation of these three families of ligands studied here is given in Scheme 1, with N atoms of the ligands numbered. Previous UV-vis spectrophotometric study[23] reported that Am(III) prefer to form 1:1 and 1:2 complexes with HBTP more than those of the trivalent lanthanides (La^{3+}, Nd^{3+}, Eu^{3+}, Tb^{3+}, Er^{3+}). To evaluate the stability of these complexes, here we also studied the complexation reaction of BTP, hemi-BTP and TPY complexes in different stoichiometric ratios of the metal atom and the ligands, ranging from 1:1 to 1:3, with the presence of nitrate ions and water molecules in the first-coordination-shell of Am^{3+}.

$[BTP-Am]^{3+}$ $[hemi-BTP-Am]^{3+}$ $[TPY-Am]^{3+}$

R=H, Ethyl, MeOPh, CyMe$_4$, CF$_3$
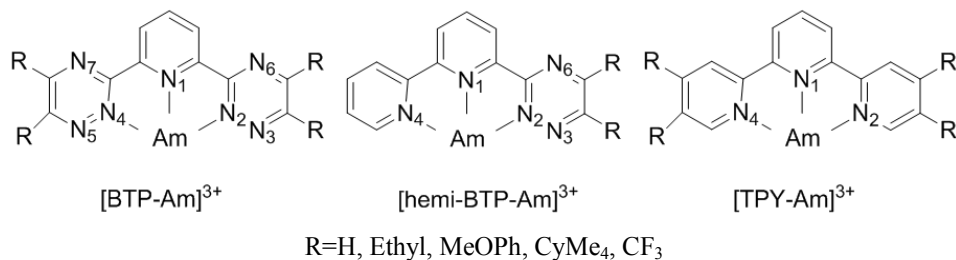
Scheme 1 The BTP, hemi-BTP and TPY ligands and their complexation with Am^{3+} cation.

As all three ligands are possible to exist in their protonated forms under highly acidic conditions, their conformational flexibility and their binding affinity with An^{3+} may be influenced by their protonation states, as shown by Wipff et al. in their study[24] of BTBPs. In an earlier work, the basicity order of R–BTPs was reported[25] to be same as that of R–pyridines in the gas phase, while it is easier to be protonated in apolar or weakly polar media with much higher protonation energy. In this work, we have also calculated the protonation energies of these ligands to evaluate how difficult for them to adopt a conformation that best fits their coordination with An^{3+}, which should be however in their deprotonated states.

2. Methods

Studies on the complexes of BTBPs with Am(III)[22, 26, 27] have shown that B3LYP[28-30] in combination with the small-core ECPs can give reliable predictions of chemical properties for actinides. In this work, the hybrid B3LYP functional implemented in the Gaussian 09 program[31] were used to perform all geometry optimizations. The inner 60 core electrons of the Am atom were treated by the Stuttgart–Dresden quasi-relativistic Effective Core Potential (ECP),[32] in combination with the corresponding basis sets with a segmented contraction scheme for the valence shells.[33, 34] The electronic configuration of Am(III) in its septet state was adopted in the calculations of the ground state properties of its complexes.[15] For other atoms, the standard Pople-style polarized valence double-ζ 6-31G(d) basis set[35] was used for optimization and frequency calculations to ensure that the obtained stationary points were minima on the potential energy surface. The composite basis set is labeled as BS1. To refine energies, the more extended, polarized valence triple-ζ 6-311G(d,p) basis set[36], which is labeled as BS2, was used to treat the atoms other than Am in single point calculations of the optimized 1:1 complexes and hydrated metal ions to describe the nonmetal atoms.

The Polarizable Continuum Model (PCM) model[37] was employed to take into account solvation effect in water. All energies reported here include zero-point energy (ZPE) correction, Gibbs free energies were also calculated at the same level, which include ZPE correction, thermal energy correction and translational, rotational and vibrational corrections. For complexation reactions, ΔE_{cf} and ΔG_{cf} represents the binding electronic energy and Gibbs free energy of the Am(III) complexes. The subscript "g" and "s" denote values calculated in the gas phase and in aqueous solution, respectively. The nature of the actinide-ligand bond was

analyzed by means of NPA charge distribution and electron density, as well as the QTAIM topological analysis of Bader.[38, 39] Multiwfn 3.2[40] was used to perform the AIM analysis. The effective charges on atoms, which are used to identify qualitatively the ionic interaction in complex formation while the overlap population of a bond were also obtained to analyze the ionic interaction qualitatively and the degree of covalent interaction respectively, as proposed in previous work.[14]

For model systems, the possible complexation reactions of Am(III) with BTP, hemi-BTP and TPY in nitric acid solutions were studied, and the thermodynamic properties were discussed in detail. The stoichiometric ratios of metal-to-ligand from 1:1 to 1:3 were all considered for BTP, hemi-BTP and TPY. For the sake of saving computational cost, only 1:1 complexes, i.e. $[ML]^{3+}$ and $ML(NO_3)_3$, were considered when investigating the influence of substituents on the complexation ability of ligands. The protonation energies E_{prot} of ligands were calculated according to eqn. (1):

$$L + [H_3O]^+ \rightarrow [L\text{-}H(H_2O)]^+ \quad (1)$$

3. Results and discussion

3.1 Protonation of BTP, hemi-BTP and TPY in water.

The tridentate N-donor ligands are conformationally flexible, and the conformations of BTP and hemi-BTP have been studied in the gas phase.[8, 41] In these ligands, the heteroatom sites may display distinct basicity depending on their location in the ring. To evaluate the protonation effect on the metal-to-ligand binding energies of different conformations, the protonation energies of ligands were calculated with solvent effect included by using the PCM model.

3.1.1 Conformations adopted by the free BTP, hemi-BTP and TPY. The relative energies of the conformations are presented in Scheme 2, and the binding energies of these conformers with Am[3+] at BS1 and BS2 levels are both collected in Table 1.
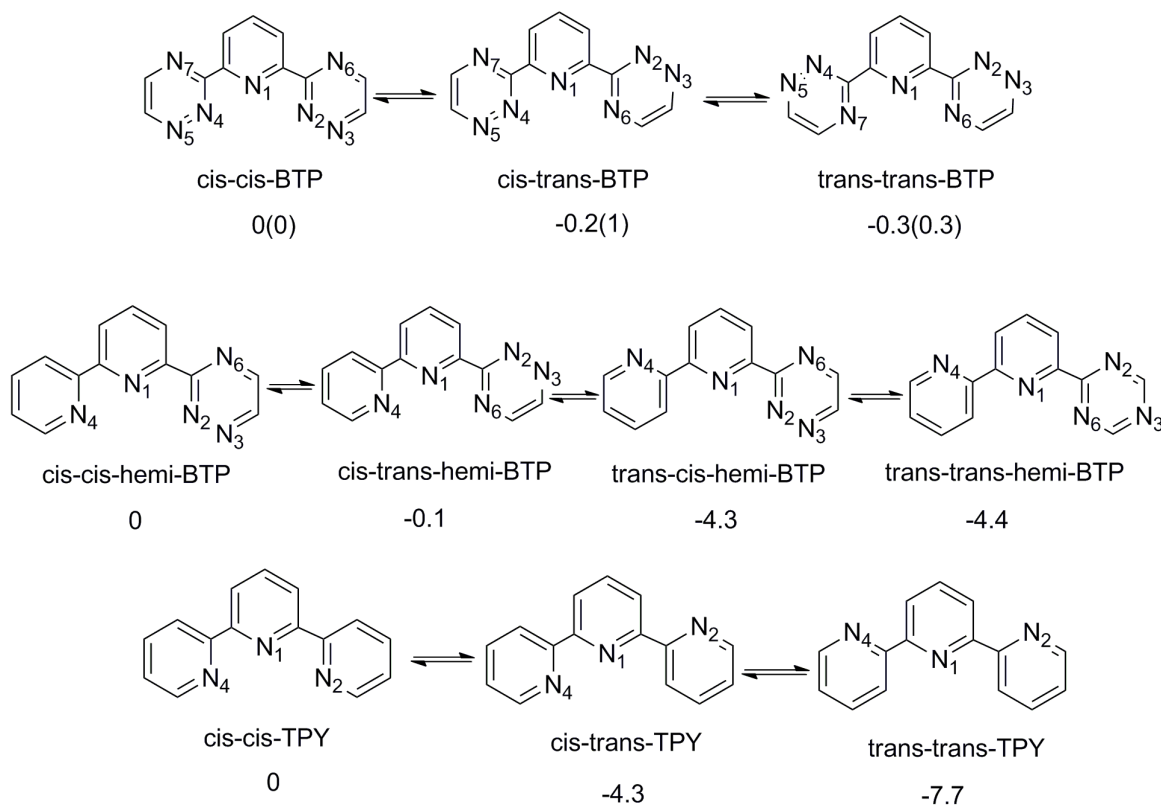
Scheme 2. The relative energies (kcal mol^{-1}) of possible BTP，hemi-BTP and TPY conformations obtained at the B3LYP/BS2 level. Data in parenthese are from Ref.[41].

In aqueous phase, BTP may adopt three possible conformations, i.e. *cis-cis*, *cis-trans* and *trans-trans* as shown in Scheme 2. The small energy difference of the three BTP conformations in aqueous solution obtained at the B3LYP/BS2 level implies an equilibrium may exist among them. This is qualitatively consistent with the results of Hudson et.al.[41] (values in bracket in Scheme 2). Though all three conformers may appear as tridentate ligands, the *cis-cis*-BTP binds to the Am^{3+} the strongest and the *trans-trans*-BTP the weakest, with a free energy difference of 6.1 kcal mol^{-1} between their binding energies.

There are four possible conformations for hemi-BTP, and the one with the lowest energy is the *trans-trans* conformation which is more stable than the *trans-cis* one by only 0.1 kcal mol^{-1} in energy. In contrast the *cis-trans* conformation is 4.3 kcal mol^{-1} higher in energy for the unfavourable interaction between two adjacent meso-hydrogen atoms, which causes the rings to twist away from co-planarity. The *cis-cis* conformation is calculated to have least stability among the four conformations.

Note that the *trans-trans* and the *trans-cis* conformers can only work as bidentate or unidentate ligands, thus not compete against the *cis-cis* and the *cis-trans* conformers towards

their complexation with metal ions thermodynamically. This means that to form the coordination complex in aqueous solution, a conformation transition from the *trans-trans* or the *trans-cis* conformations of hemi-BTP to its *cis-cis* or *cis-trans* conformations. In view of binding energy, as seen in Table 1, the *cis-cis* complex is more stable than the *cis-trans* complex by 3.7 kcal mol^{-1}.

Table 1. Calculated binding energies (kcal mol^{-1}) for the $[AmL]^{3+}$ complexes.

Conformations	ΔE/BS1	ΔG/BS1	ΔE/BS2	ΔG/BS2
cis-cis-BTP	-23.8	-12.8	-17.7	-6.7
cis-trans-BTP	-20.9	-10.3	-16.7	-6.0
trans-trans-BTP	-14.7	-4.4	-10.9	-0.6
cis-cis-hemi-BTP	-30.9	-21.1	-25.8	-15.9
cis-trans-hemi-BTP	-27.0	-17.1	-22.1	-12.2
cis-cis-TPY	-34.2	-25.1	-28.5	-19.4

For TPY, there are three possible conformations, as shown in Scheme 2. The *trans-trans* conformation is much more stable than *cis-cis* conformation by an energy of 7.7 kcal mol^{-1} due to more locally distributed hydrophilicity/hydrophobicity in the latter while more equally distributed in the former. Note that, however, only the *cis-cis*-TPY can form the thermodynamically much more stable tridentate complex $[AmL]^{3+}$, while *cis-trans*-TPY and *trans-trans*-TPY are present as bidentate or monodentate ligands respectively.

The above analysis shows that only BTP can easily realize the conformation transitions between its thermodynamically more stable conformation and the one favoring to complex with metal ions. This may suggest that the molecular flexibility is an important contributor in their interaction with An(III)/Ln(III).

3.1.2 Protonation. The protonation of extractants may occur during the extraction process which is in general carried out in nitric acid, and the protonation of BTP has been investigated.[25, 41] In the present work, in order to find the influence of protonation on their conformational preferences, the isomers of these N-tridentate ligands were protonated and optimized. As the three BTP isomers have similar energies according to our calculations, the *cis-cis*-BTP isomer was chosen as an example. Four different nitrogen atoms that potentially could be protonated, as shown in Scheme 3. It is noticeable that the most preferential protonation site is the central pyridine atom N_1, and the structure is stabilized by hydrogen bonding interactions between the N-H group and the nitrogen atoms on the two lateral rings. Thus, the central pyridine N_1 of protonation will be considered throughout the following study.
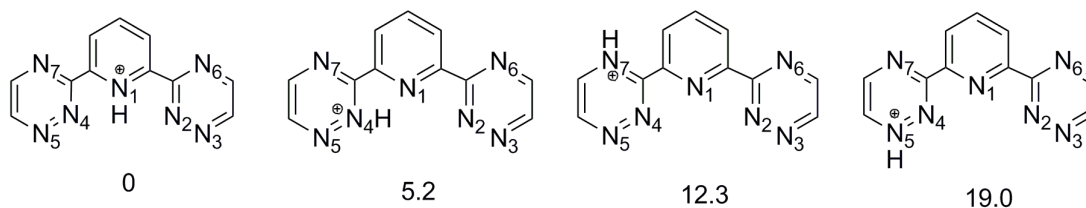
Scheme 3. Protonation energies (kcal mol^{-1}) at four N sites of *cis-cis*-BTP.

From Table 2, it seems likely that there is a facile conversion among the three BTP protonation conformations. For hemi-BTP, It is noted that the protonation free energies for the protonated species (*cis-cis* < *cis-trans* < *trans-cis* < *trans-trans*) is the exactly opposite to its deprotonated form (*cis-cis* > *cis-trans* > *trans-cis* > *trans-trans*). Note that protonation of the molecules does not favor their *cis-cis* conformations which is however required for binding to Am^{3+}. Protonation energy of TPY conformations show the same trend, i.e. *cis-cis* < *cis-trans* < *trans-trans*, both at the BS1 and BS2 levels.

Compared to the other two types of the ligands, TPY has stronger propensity to be protonated, and the protonation energy of their *cis-cis* conformation, which is required to complex to metal ion, decreases in the order of *cis-cis*-TPY > *cis-cis*-hemi-BTP > *cis-cis*-BTP, consistent with their experimental values of pKa which is 5.2 for pyridine while negative for 1,2,4-triazine.[42] The higher deprotonation energy required for TPY and hemi-BTP could significantly inhibit their conversion to the tridentate conformation during the extraction process.

Table 2. Protonation energies (kcal mol^{-1}) of BTP, hemi-BTP and TPY with the N$_1$ atom of the central pyridine protonated.

Conformations	BS1				BS2			
	ΔE	ΔG	$\Delta(\Delta E)$	$\Delta(\Delta G)$	ΔE	ΔG	$\Delta(\Delta E)$	$\Delta(\Delta G)$
cis-cis-BTP	-37.3	-26.4	0.0 (0.0)[a]	0.0	-34.3	-23.4	0.0	0.0
cis-trans-BTP	-37.1	-26.5	0.2 (0.4)[a]	-0.1	-34.2	-23.6	0.1	-0.2
trans-trans-BTP	-37.7	-27.4	-0.4(-0.3)[a]	-1.0	-34.3	-24.0	0.0	-0.6
cis-cis-hemi-BTP	-41.7	-31.3	-4.3(0.0)[b]	-4.1	-38.6	-28.1	-4.5	-4.3
cis-trans-hemi-BTP	-40.8	-30.7	-3.4(0.82)[b]	-3.5	-37.7	-27.5	-3.6	-3.7
trans-cis-hemi-BTP	-38.3	-27.8	-0.9(4.69)[b]	-0.6	-35.1	-24.5	-1.0	-0.7
trans-trans-hemi-BTP	-37.4	-27.2	0.0 (6.35)[b]	-0.0	-34.1	-23.8	0.0	0.0
cis-cis-TPY	-46.7	-36.9	-11.2	-11.8	-43.0	-33.2	-10.2	-10.9
cis-trans-TPY	-41.9	-32.0	-6.4	-6.9	-38.2	-28.3	-5.4	-6.0
trans-trans-TPY	-35.5	-25.1	0.0	0.0	-32.8	-22.3	0.0	0.0

[a]The values in the parentheses were calculated using COSMO method with TZP level from Ref. [41]

[b]The values in the parentheses were calculated at HF/6-31+G* level from Ref.[8]

3.2 Substitution effect and Am-N bond nature in [AmL]$^{3+}$ complexes.

3.2.1 Electronic Structures. We choose R=Ethyl, MeOPh (Methoxyphenyl), CyMe$_4$, CF$_3$ to assess the influence of the lateral substituted rings. To evaluate the charge transfer between the ligands and Am(III), the atomic charge of Am^{3+} (q_M), and the group charges of the central and lateral rings (including substituents), i.e. the summation of effective atomic charges of the central pyridine ring (Q_c), the lateral triazine ring (Q_{taz}), and the lateral pyridine ring (Q_{Lpy}), were determined. The NPA charges the free ligands L and [AmL]$^{3+}$ complexes carry obtained from gas phase calculations are presented in Table 3.

Table 3. Calculated atomic q_M and group charges Q_c, Q_{taz}, and Q_{Lpy} of the free ligand L and the corresponding [AmL]$^{3+}$ complexes in the gas phase.

L	free ligand charges			[AmL]$^{3+}$ charges			
	Q_c	Q_{taz}	Q_{Lpy}	Q_c	Q_{taz}	Q_{Lpy}	q_M
BTP	0.052	-0.026	-	0.308	0.231	-	2.230
hemi-BTP	0.023	-0.031	0.008	0.257	0.242	0.231	2.270
TPY	-0.005	-	0.003	0.270	-	0.278	2.174
C2-BTP	0.032	-0.016	-	0.254	0.291	-	2.165
C2-hemi-BTP	0.014	-0.018	0.004	0.224	0.358	0.201	2.212
C2-TPY	-0.013	-	0.007	0.215	-	0.359	2.066
MeOPh-BTP	0.026	-0.013	-	0.089	0.590	-	1.731
MeOPh-hemi-BTP	0.010	-0.013	0.003	0.102	1.028	0.120	1.750
MeOPh-TPY	-0.009	-	0.004	0.040	-	0.627	1.705
CyMe4-BTP	0.029	-0.014	-	0.166	0.359	-	2.117
CyMe4-hemi-BTP	0.012	-0.016	0.004	0.196	0.484	0.184	2.136
CyMe4-TPY	-0.014	-	0.007	0.193	-	0.410	1.988
CF3-BTP	0.095	-0.047	-	0.320	0.221	-	2.239
CF3-hemi-BTP	0.048	-0.064	0.016	0.264	0.224	0.236	2.276
CF3-TPY	0.036	-	-0.018	0.289	-	0.260	2.191

In all of the free R-BTPs and R-hemi-BTPs, the group charges of the three rings are close to 0 with minor difference that the group charge of the pyridine ring(s) (Q_c, Q_{Lpy}) is positive and that of the lateral triazine rings (Q_{taz}) is negative because of the presence of additional nitrogen atoms. The additional nitrogen atoms in the 1,2,4-triazine moiety render the 1,2,4-triazine weaker ligand than pyridine, which is beneficial for the separation of An/Ln. For free ligands R-TPYs, Q_c is negative when R is an electron donating group while positive when R=CF$_3$ which has strong electron-withdrawing ability.

In the complexes $[AmL]^{3+}$, the interaction between the two moieties corresponds mainly to ionic interactions but with minor contribution of covalency, and the quantity of the charge transfer between Am(III) and ligands displays dependence on the electronic property of the substituents R on the lateral rings, i.e. the stronger the electron donating ability of R, the more charge transfer, and follows the order R = MeOPh > $CyMe_4$ > Ethyl > H > CF_3 in the gas phase. In all of the complexes, the atomic charge on Am(III) is in the range of 2.16 ~ 2.28e, except for the case of R= MeOPh, which is a good electron donor and in the complex the Am(III) carries 1.7e charge. Concerning the effect of 1,2,4-triazine of lateral rings, the transferred charges decrease in the order of R-TPYs > R-BTPs > R-hemi-BTPs, indicating that the electron-donating groups make the lateral rings lose more electrons during the coordination process. In aqueous solution, the transferred charges are smaller than that in the gas phase (see Table S1 of Supporting Information), which showed that the solvent effects reduced the transferred charges from ligands to Am.

3.2.2 Geometry. To explore the M-L bonding nature, the calculated metal-ligand bond lengths, the Mayer bond orders (BOPs), and the bond overlap populations (BOPs) in $[AmL]^{3+}$ complexes were analyzed and collected in Table 4.

Table 4. Calculated Am-N distances (d_{Am-N}, in Å), Mayer bond order (MBO) and bond overlap populations (BOPs) in $[AmL]^{3+}$ complexes in the gas phase.

L	d_{Am-N}			MBO			BOPs		
	N_1	N_2	N_4	N_1	N_2	N_4	N_1	N_2	N_4
BTP	2.58	2.32	-	0.41	0.48	-	0.27	0.28	-
hemi-BTP	2.49	2.31	2.37	0.48	0.49	0.57	0.30	0.29	0.31
TPY	2.44	2.42	-	0.47	0.50	-	0.28	0.27	-
C2-BTP	2.58	2.29	-	0.40	0.51	-	0.27	0.31	-
C2-hemi-BTP	2.50	2.27	2.39	0.46	0.52	0.54	0.29	0.31	0.31
C2-TPY	2.46	2.43	-	0.45	0.49	-	0.27	0.27	-
MeOPh-BTP	2.57	2.47	-	0.34	0.37	-	0.23	0.25	-
MeOPh-hemi-BTP	2.54	2.50	2.51	0.36	0.35	0.40	0.24	0.24	0.24
MeOPh-TPY	2.51	2.50	-	0.38	0.41	-	0.25	0.25	-
CyMe4-BTP	2.44	2.40	-	0.43	0.44	-	0.26	0.27	-
CyMe4-hemi-BTP	2.50	2.32	2.42	0.44	0.47	0.51	0.28	0.28	0.29
CyMe4-TPY	2.45	2.45	-	0.43	0.46	-	0.27	0.28	-
CF3-BTP	2.59	2.33	-	0.41	0.47	-	0.27	0.28	-
CF3-hemi-BTP	2.49	2.31	2.37	0.48	0.49	0.57	0.30	0.29	0.31
CF3-TPY	2.45	2.43	-	0.47	0.49	-	0.28	0.27	-

In view of Am-N bond length, the Am-N_1 bond length is significantly longer than that of

Am-N_2 in all BTP and hemi-BTP complexes, as seen in Table 4, and the bond order is smaller than that of Am-N_2. The presence of electron donating substituent on the lateral rings, MeOPh-, diminishes the difference between the two bonds.

Regarding to the bond overlap population (BOP), a typical covalent single bond such as C-H bond has a value within the range of 0.8 - 0.9. In the case of Am-N bond studied here, the value is in the range of 0.24 - 0.30, and the very small BOP values of Am-L bonds indicate minor contribution of covalency. Given the relatively short Am-L bond distance, the MBO values of around 0.4, and the charge transfer between Am and the ligands, it is conceivable that the ionic interaction may dominate the M-L interaction in the Am (III) complexes.

3.2.3 Thermodynamics. The binding energies ΔE_{cf} and Gibbs free energies ΔG_{cf} of $[AmL]^{3+}$ in the gas phase and aqueous phase are presented in Figure 1.

The values of ΔE_{cf} and ΔG_{cf} of ligands differing in their terminal substituents show similar trends in the $[AmL]^{3+}$ complexes. In the gas phase, the binding energies of $[AmL]^{3+}$ for L=R-TPYs are more negative than that for L=R-BTPs. When the solvent effect is taken into account, the binding free energies decrease to be less than 40 kcal mol^{-1} for the complexes $[AmL]^{3+}$, with L=R-TPYs more stable than that for R-BTPs and R-hemi-BTPs. It is noted that the thermal stability of the $[AmL]^{3+}$ complexes studied here increases as the electron-donating ability of the substituents increases, in the order R = MeOPh > $CyMe_4$ > Ethyl > H > CF_3 in the gas phase, which is consistent with the above NPA charges. In the solution, the ligand BTP with R=Ethyl has stonger propensity to bind with Am(III) than with $CyMe_4$.
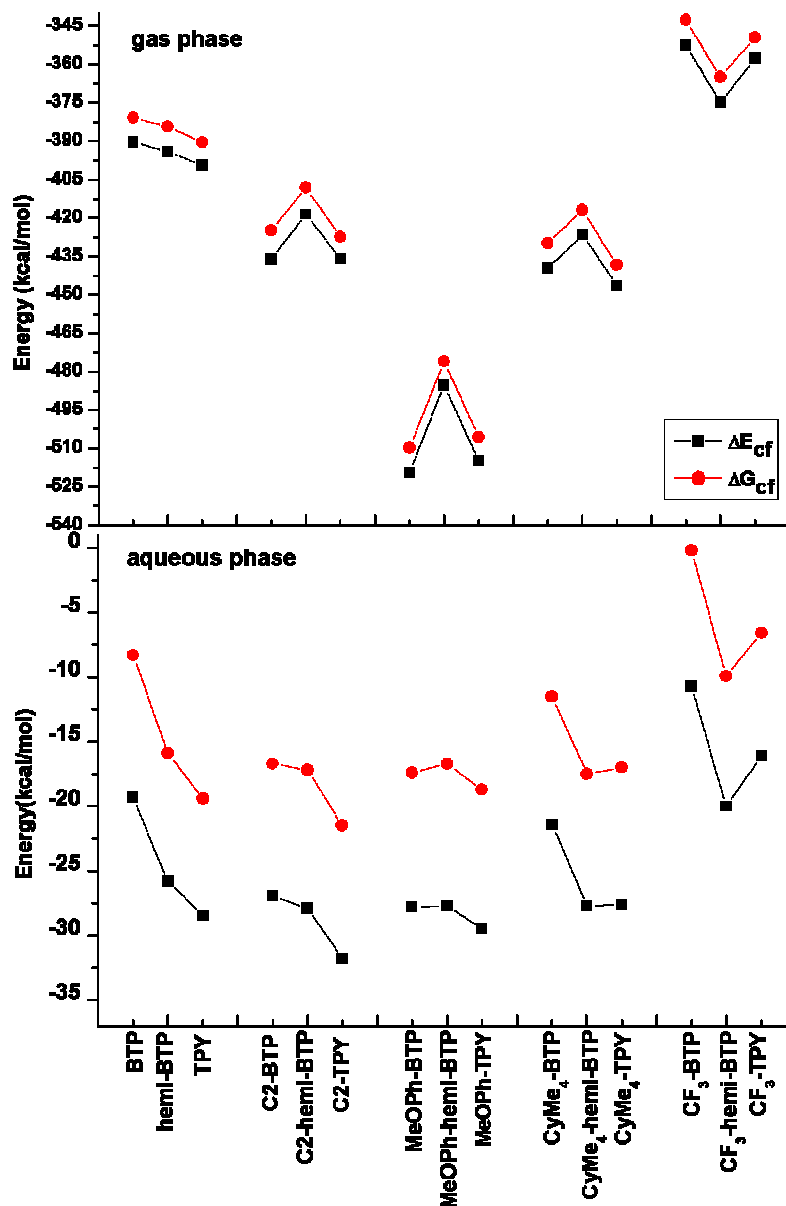
Figure 1. The binding energies and Gibbs free energies (kcal mol^{-1}) of the [AmL]$^{3+}$ complexes in the gas phase and aqueous solution calculated at the B3LYP/BS2 level.

3.3 Influence of nitrate ion in [AmL(NO₃)₃] complexs

3.3.1 Structure. In condensed phase, the presence of counter-ions and solvents may have a noticeable impact on formation of M-L complexes in aqueous solution. To understand the role of nitrate ions in the complexation of Am(III) with organic ligands, the geometries of AmL(NO$_3$)$_3$ complexes, where L denotes R-BTPs, R-hemi-BTPs and R-TPYs, were optimized and their thermodynamic stabilities were compared. The Am-N bond length, averaged Am-O

bond length and the corresponding Mayer bond order are collected in Table 5.

Table 5. Calculated Am-N distances (d_{Am-N}, in Å), averaged Am-O bond lengths (d_{Am-O}, in Å), Mayer bond order (MBO) of [AmL(NO$_3$)$_3$] complexes in the gas phase.

L	d_{Am-N}					MBO				
	N_1	N_2	N_4	O_i^a	O_o^a	N_1	N_2	N_4	O_i	O_o
BTP	2.72	2.65	-	2.45	2.49	0.18	0.17	-	0.37	0.35
hemi-BTP	2.70	2.62	2.65	2.47	2.49	0.19	0.18	0.23	0.34	0.35
TPY	2.65	2.64	-	2.47	2.49	0.21	0.24	-	0.34	0.34
C2-BTP	2.71	2.63	-	2.46	2.49	0.18	0.19	-	0.36	0.36
C2-hemi-BTP	2.68	2.61	2.65	2.47	2.49	0.20	0.20	0.22	0.33	0.35
C2-TPY	2.65	2.63	-	2.48	2.50	0.22	0.25	-	0.34	0.34
MeOPh-BTP	2.73	2.62	-	2.47	2.49	0.18	0.20	-	0.35	0.35
MeOPh-hemi-BTP	2.69	2.60	2.65	2.47	2.49	0.20	0.20	0.23	0.35	0.34
MeOPh-TPY	2.65	2.63	-	2.48	2.50	0.22	0.25	-	0.33	0.34
CyMe4-BTP	2.71	2.63	-	2.46	2.49	0.18	0.20	-	0.35	0.35
CyMe4-hemi-BTP	2.68	2.61	2.65	2.48	2.49	0.20	0.20	0.22	0.34	0.35
CyMe4-TPY	2.65	2.62	-	2.48	2.50	0.22	0.25	-	0.33	0.34
CF3-BTP	2.74	2.68	-	2.44	2.48	0.17	0.16	-	0.38	0.35
CF3-hemi-BTP	2.69	2.67	2.64	2.46	2.48	0.19	0.17	0.23	0.34	0.35
CF3-TPY	2.67	2.66	-	2.46	2.48	0.20	0.22	-	0.35	0.35

[a] O_i and O_o denote the coordinating oxygen atoms of the in- and out-of-plane molecules, respectively.

Coordination of nitrate ions in the gas phase makes the Am-N bond lengths elongated by about 0.2-0.3 Å than the corresponding values of [AmL]$^{3+}$. In the presence of NO$_3^-$, the Am-N$_2$ bonds are still shorter than the Am-N$_1$ bonds. Meanwhile, in the complexes of hemi-BTPs, the Am-N$_2$ (1,2,4-triazine) bond is also shorter than Am-N$_2$ (lateral pyridine) except for the case with R = CF$_3$. In addition, the presence of NO$_3^-$ in the first coordination shell also diminishes the lateral substituent effects. The Am-N bond lengths of CF$_3$-BTP complex are a little longer than other substituted ligands, owing to the stronger electron-accepter ability of CF$_3$.

The inner-sphere nitrate ions also modulate the M-L bond mode. As seen in Table 5, Mayer bond orders of Am-N decrease significantly in the AmL(NO$_3$)$_3$ complexes in comparison with those in [AmL]$^{3+}$, and the bond orders of Am-O are much larger than that of Am-N. In aqueous solution, unlike the [AmL]$^{3+}$ complexes, Am-N and Am-O are a little shorter and the corresponding bond orders are slightly larger in the AmL(NO$_3$)$_3$ complexes, which suggest more covalence feature of the metal-ligand bonds in aqueous phase.

3.3.2 Thermodynamics. The thermodynamic stability of AmL(NO$_3$)$_3$ complexes were

evaluated by defining the binding free energy as

$$\Delta G = G(AmL(NO_3)_3) - G(Am^{3+}) - G(L) - 3 \times G(NO_3^-)$$

Figure 2 show the calculated binding energies ΔE_{cf} and ΔG_{cf} of $AmL(NO_3)_3$ in both gas phase and aqueous phase, which are much higher than those of $[AmL]^{3+}$. Among the ligands studied here the corresponding binding energies do not differ much. However, it is still noticeable that the complexes with L=R-TPYs are more stable than with L=R-BTPs, which agrees well with that of the $[AmL]^{3+}$ complexes. The thermodynamic stability of $AmL(NO_3)_3$ studied here slightly increases as the electron-donating ability of the substituents increases. The R-BTPs complexes with R=MeOPh or $CyMe_4$ have similar binding strength.
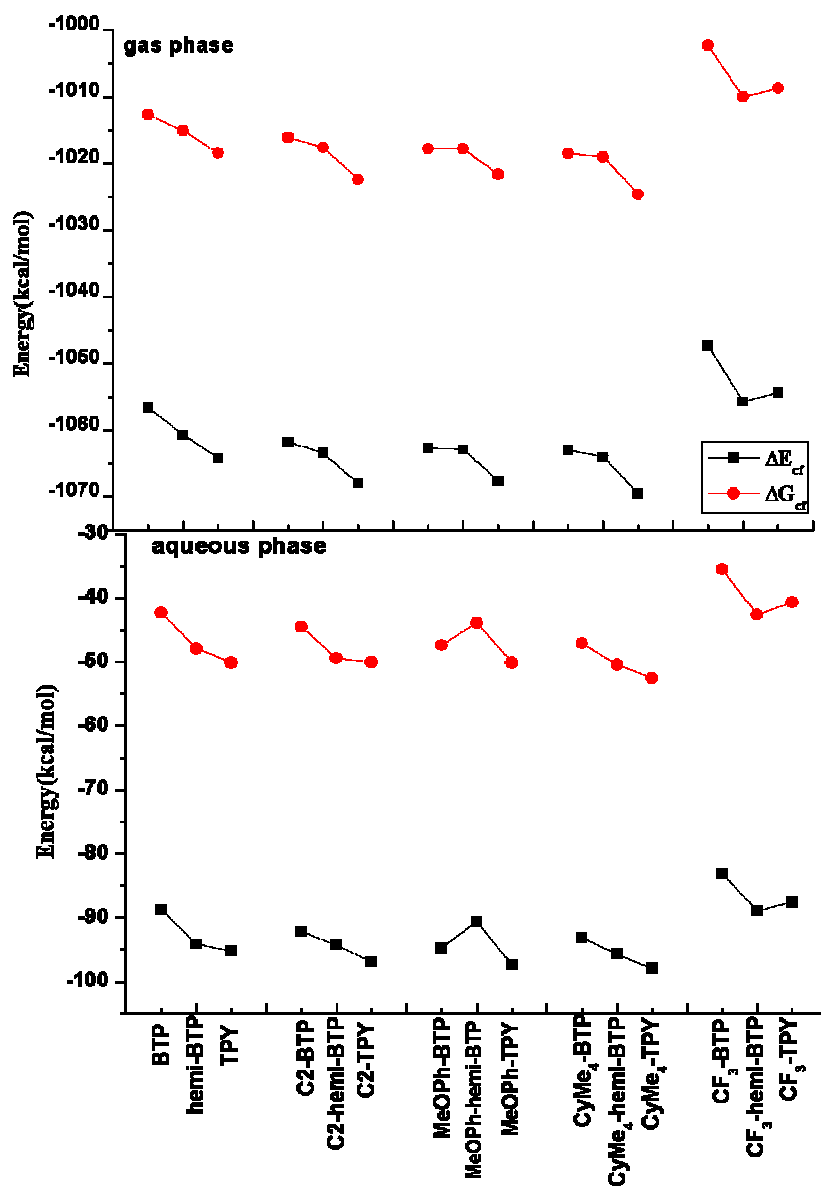
Figure 2. The binding energies and Gibbs free energies (kcal mol^{-1}) of the complexes [AmL(NO$_3$)$_3$] in the gas phase and aqueous solution calculated at the B3LYP/BS2 level.

3.4 QTAIM Topological Analysis of Gas-Phase Electron Densities.

The bonding properties can be further supported by the electron density using the QTAIM method, as reported in Supporting Information, Table S7. In the framework of AIM, a chemical bond may be characterized by four descriptors, i.e. the electron density at the bond critical point (BCP) and its Laplacian $\nabla^2\rho_b$, and the total electronic energy density H_b. H_b is negative for

16

interactions with significant sharing of electrons, and its magnitude reflects the "covalence" of the interaction. The more negative the value, the stronger the covalent interaction.

For the complex $[AmL]^{3+}$, the Laplacian $\nabla^2\rho_b$ is positive with $\rho \approx 0.05 \sim 0.09$ e$^-$/bohr^3, close to 0.08 e$^-$/bohr^3 calculated for the LiF molecule,[43] suggesting only minor electron accumulation between Am and the ligands. According to Bader et al.[44] the value of 0.10 e$^-$/bohr^3 may be looked as an upper bound of a closed-shell interaction, suggesting the Am-N bond in $[AmL]^{3+}$ is highly ionic. This is supported by the total energy density value which is negative while close to zero, and is also consistent with the low Mayer bond order, as discussed in the previous section. For the complex $[AmL(NO_3)_3]$, Am-N bonds are predominantly ionic, which is also supported by small ρ values, $\nabla^2\rho_b > 0$ and $H_b \approx 0$. It is difficult to see the substitution effects of the ligands from the topological parameters due to the weak covalent interaction.
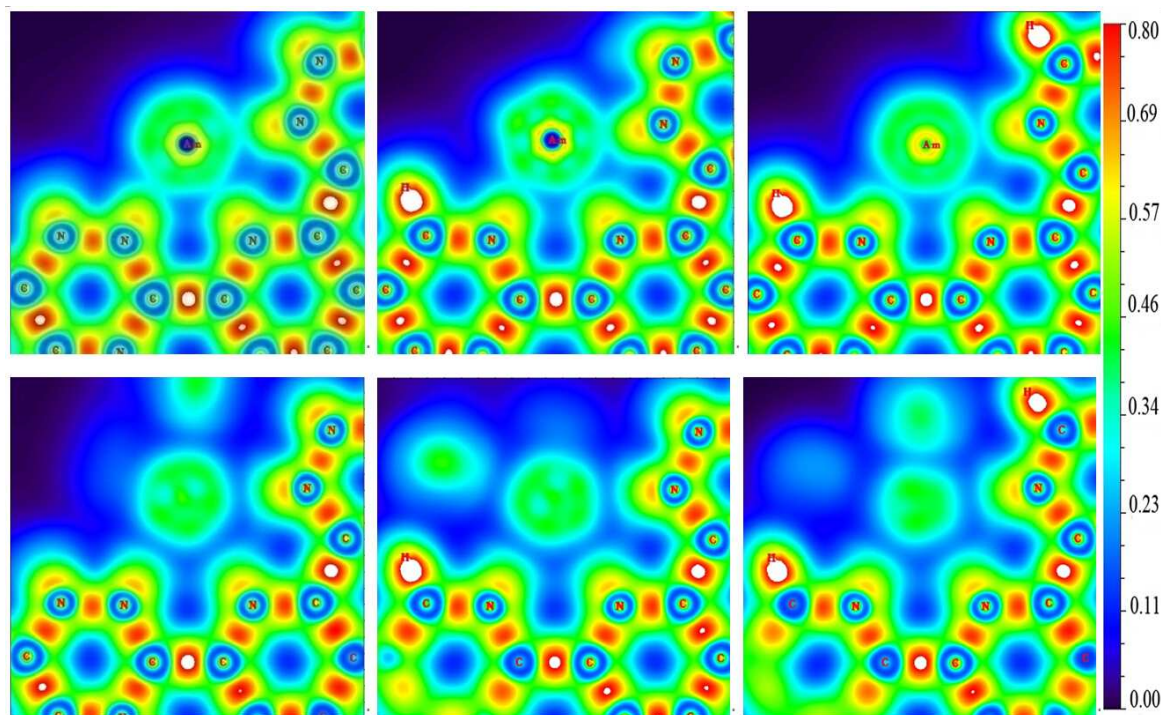
Figure 3. The localized orbital locator (LOL) of $[AmL]^{3+}$ (upper) and $AmL(NO_3)_3$ (lower) with L=CyMe$_4$-BTP (left), CyMe$_4$-hemi-BTP (middle) and CyMe$_4$-TPY (right)

The topological methodology of localized orbital locator (LOL)[45] for the complexes $[ML]^{3+}$ and $ML(NO_3)_3$ when L=CyMe$_4$-BTP, CyMe$_4$-hemi-BTP and CyMe$_4$-TPY were shown in Figure 3. LOL is also a bonding descriptor, and may reflect atomic shell structure. It simply shows when localized orbitals overlap, i.e. forming a bond, the gradient of which reaches a

maximum, thus provides a simple and recognizable pattern of a chemical bond.[46] As seen in Figure 3, the Am-L orbital interaction is obviously weak in the complex $[ML]^{3+}$, and the presence of nitrate ions in the complexes diminishes the weak orbital interaction between metal ion and ligands further in $ML(NO_3)_3$. Note that for the three types of tridentate ligands, the localization index around Am-N of BTP ligand is slightly higher than that around that of TPY ligand, suggesting slightly more covalency in Am-N bond of BTP.

3.5 Frontier orbitals of L and $[ML_n]^{3+}$ (n=1, 3) from Mulliken population analysis

3.5.1 Ligands. The frontier orbitals of the ligands BTP, hemi-BTP and TPY are shown in Figure 4. It is clear that there are high similarities between the orbitals of BTP and hemi-BTP. The Highest Occupied Molecular Orbital (HOMO) has σ character between nitrogen and carbon atoms while the lowest unoccupied molecular orbital (LUMO) is found to be a π* orbital. The orbitals of the lateral pyridine ring make no contribution in the frontier orbitals of hemi-BTP. The HOMO of TPY is a π orbital contributed by the three pyridine rings. In view of the symmetries of frontier orbitals, BTP may work as better σ-donor and π-acceptor, while TPY requires molecular deformation to adapt the coordination interaction when bound to metal ion.

The HOMO-LUMO gap has been proposed to be used as a measure of the absolute hardness of a molecular system.[47] In Figure 4, The HOMO energy level of TPY is lower in energy than that of BTP, while the LUMO π* orbital of TPY is at higher energy level, and the HOMO-LUMO gap of BTP is calculated to be much smaller than that of TPY, suggesting a lower hardness of BTP than that of TPY, which may enable BTP better selectivity of towards the Ln/An separation than TPY.
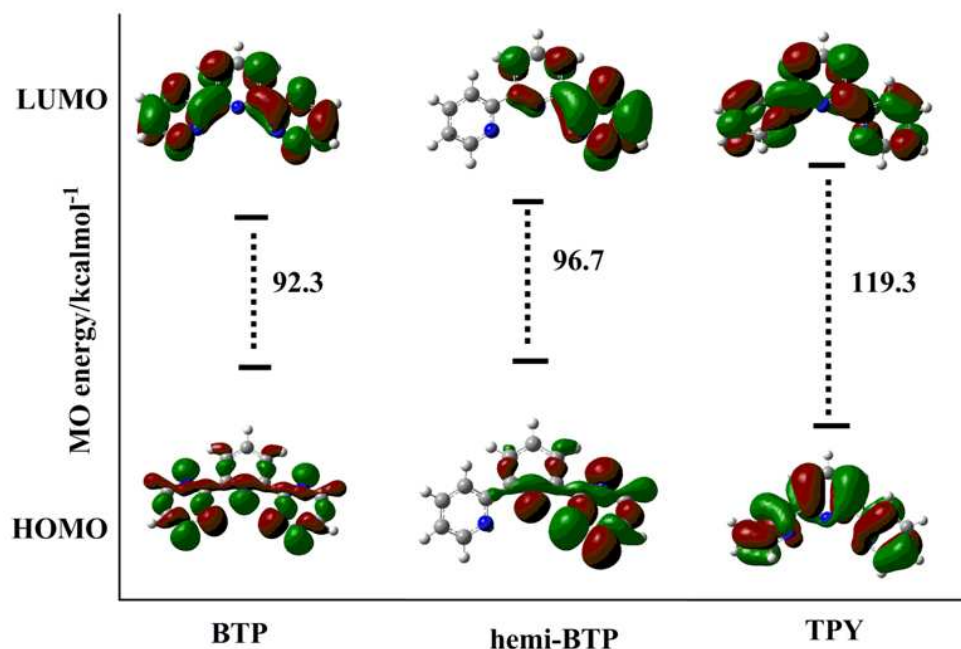
Figure 4. The diagram of frontier orbitals and HOMO-LUMO energy gaps of BTP, hemi-BTP and TPY in the gas phase. The isosurface value of molecular orbitals is set to be 0.02 au.

3.5.2 [AmL]$^{3+}$ complexes. Significant contribution of 5f orbitals was found in the frontier orbitals, and the covalent bonding in these systems can be described in terms of a ligand-to-metal donation, involving the filled ligand σ and π molecular orbitals and the vacant metal 7s, 6d and 5f orbitals and metal-to-ligand back-donation from the partially filled metal 5f orbitals involved in the metal-ligand bonding. Figure 5 presents the representative α-spin MOs of [AmL]$^{3+}$ complexes which contain contributions from both Am and the ligand moieties, including both singly occupied and doubly occupied orbitals. The contributions from the atomic orbitals of Am are tabulated in Table 6.

The frontier orbitals of complexes with BTP and hemi-BTP are similar. For the HOMO orbital of the three ligand complexes, ligand-to-metal donation is found mainly the ligand π orbitals except for 33.6% metal orbitals in TPY complexes, and there is no orbital overlap between N and Am atoms.

As shown in Figure 5, the inner occupied MOs are found to be shared by the metal and the outer rings of the ligands, each of which has less than 50% metal character. The MOs correspond to ligand to metal donation involving the ligand σ orbital and the empty metal orbitals, the 5f as well as the 6d orbitals, are active in bond formation. According to our calculations, six 5f electrons stay in the occuped orbitals of [AmL]$^{3+}$ complexes far away from

19

the fermi level, e.g. appear below HOMO-6 for the ligand hemi-BTP. In addition, metal-to-ligand back-donation takes place mainly the donation involves a singly occupied $5f$ orbital with significant contribution from the ligand, 22.1% of BTP and 23.2% of TPY. The metal-to-ligand back-donation is much stronger than ligand-to-metal donation among three ligands.
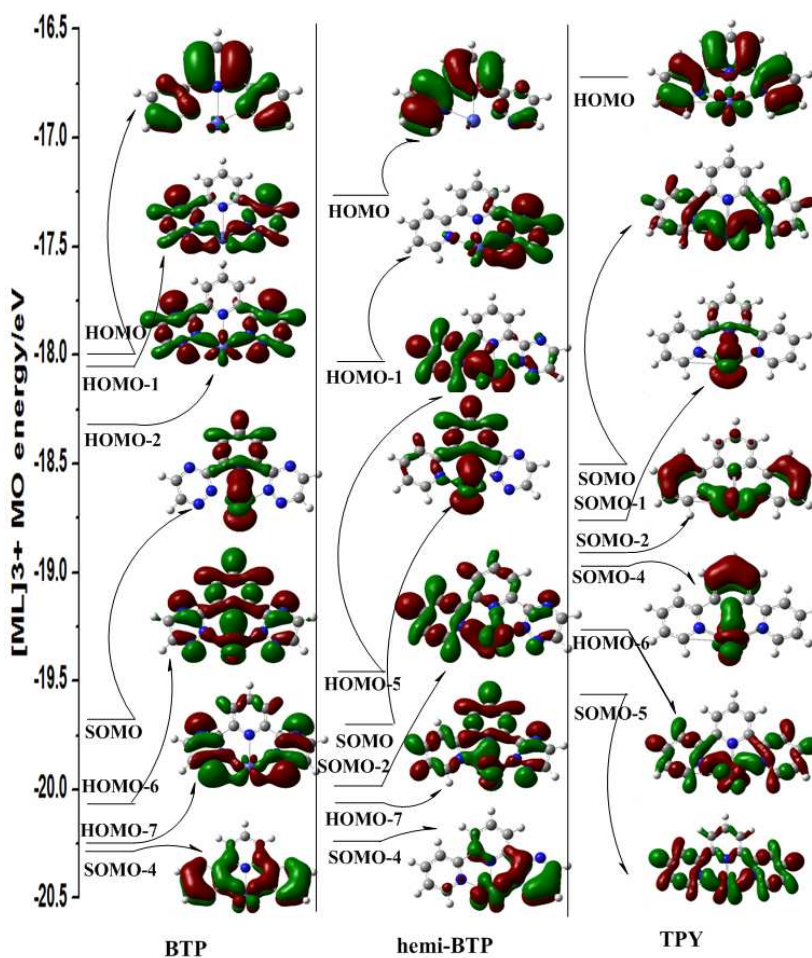
Figure 5. Representative α-Spin MOs of $[AmL]^{3+}$ in the gas phase. The corresponding contributions of Am atom are listed in Table 6. The isosurface value of MO is 0.02 au.

Table 6. Contributions (%) and Compositions (%) of Am orbitals [a] to Representative α-Spin MOs of [AmL]$^{3+}$ and [AmL$_3$]$^{3+}$.

	BTP		hemi-BTP		TPY
Orbital	M(%)	Orbital	M(%)	orbital	M(%)
[ML]$^{3+}$					
HOMO	1.3(0.6d)	HOMO	0.5	HOMO	33.6(1.1d+31.8f)
HOMO-1	5.9(4.3d)	HOMO-1	13.9(2.6d+10.7f)	**SOMO**	**76.8(3.6d+72.1f)**
HOMO-2	19.0(18.3f)	HOMO-5	44.0(4.5d+37.3f+0.8s)	**SOMO-1**	**93.3(0.7d+90.8f+1.3s)**
SOMO	**77.9(2.1d+73.8f+1.4s)**	**SOMO**	**56.0(3.6d+49.2f+2.1s)**	**SOMO-2**	**76.3(76.1f)**
HOMO-6	25(1.1d+22.4f+1.2s)	**SOMO-2**	**59.0(0.5d+58.2f)**	**SOMO-4**	**75.7(75.6f)**
HOMO-7	14.4(0.5p+11.0f+2.2d)	HOMO-7	74.4(74.3f)	HOMO-6	70.1(0.9d+68.5f)
SOMO-4	**42.8(42.5f)**	**SOMO-4**	**45.2(0.7d+43.3f+0.8s)**	**SOMO-5**	**56.9(2.1d+54.3f)**
[ML$_3$]$^{3+}$					
SOMO	**50.4(2.0d+47.8f)**	HOMO	3.8(3.7f)	HOMO	0.2
SOMO-1	**50.3(2.2d+47.5f)**	HOMO-1	4.4(4.3f)	HOMO-1	0.5
HOMO	12.0(1.2p+9.6f)	**SOMO**	**25.6(0.6d+24.6f)**	HOMO-2	1.5(1.1f)
HOMO-1	39.4(2.1d+36.8f)	HOMO-2	34.9((1.0d+33.2f)	**SOMO**	**78.3(1.7d+76.3f)**
HOMO-2	1.5	**SOMO-1**	**57.8(2.0d+55.4f)**	**SOMO-1**	**81.4(0.9d+79.6f)**
HOMO-3	14.7(2.3d+11.6f)	**SOMO-2**	**36(0.7d+34.1f)**	**SOMO-2**	**83.0(82.4f)**
HOMO-4	1.8	HOMO-3	58.0(1.3d+56f)	HOMO-3	9.7(9.2f)
HOMO-5	2.8(2.0f)	HOMO-4	26.5(0.8d+24.9f)	HOMO-4	36.2(35.6f)
HOMO-6	3.3(0.7d+0.5f+0.5s)	HOMO-5	47.1(0.6d+45.9f)	**SOMO-3**	**40.2(39.8f)**
SOMO-2	**59.3(58.9f)**	**SOMO-3**	**77.3(76.9f)**	HOMO-5	51.8(51.2f)
HOMO-7	41.8(40.7f+0.9s)	**SOMO-4**	**72(0.6d+70.6f)**	**SOMO-4**	**51.6(50.6f)**
HOMO-8	43.2(42.9f)			**SOMO-5**	**80.0(79.3f)**
SOMO-3	**83.5((83.3f)**				
SOMO-4	**80.7(80.2f)**				
SOMO-5	**84.8(84.7f)**				

[a] Only contributions greater or equal to 0.5% are reported. HOMO orbitals are doubly occupied whereas SOMO orbitals are singly occupied.

3.5.3 [AmL$_3$]$^{3+}$ complexes. For [ML(NO$_3$)$_3$], it is difficult to observe the interaction of metal and tridentate N-donor ligand due to the presence of "hard" base nitrate ion in the first coordination shell of the metal ion. If the concentration of extractant is sufficiently high, the 1:3 complexes [ML$_3$]$^{3+}$ may be obtained in the extraction process. Here the representative α-Spin frontier orbitals of the complex [AmL$_3$]$^{3+}$ are displayed in Figure 6, and the contributions and compositions of Am orbitals to these MOs are shown in Table 6.

For the ligand BTP, two 5f electrons are exposed to the outside of the doubly occupied orbitals, the 50% contribution of the metal orbitals shows metal-to-ligand donation and the overlap of the metal f orbitals and the N *p* orbitals of SOMO and SOMO-1 can be seen in Figure 6. Less orbital overlap of σ orbitals of ligand and 5f orbitals of Am(III) is observed in

doubly occupied orbitals.
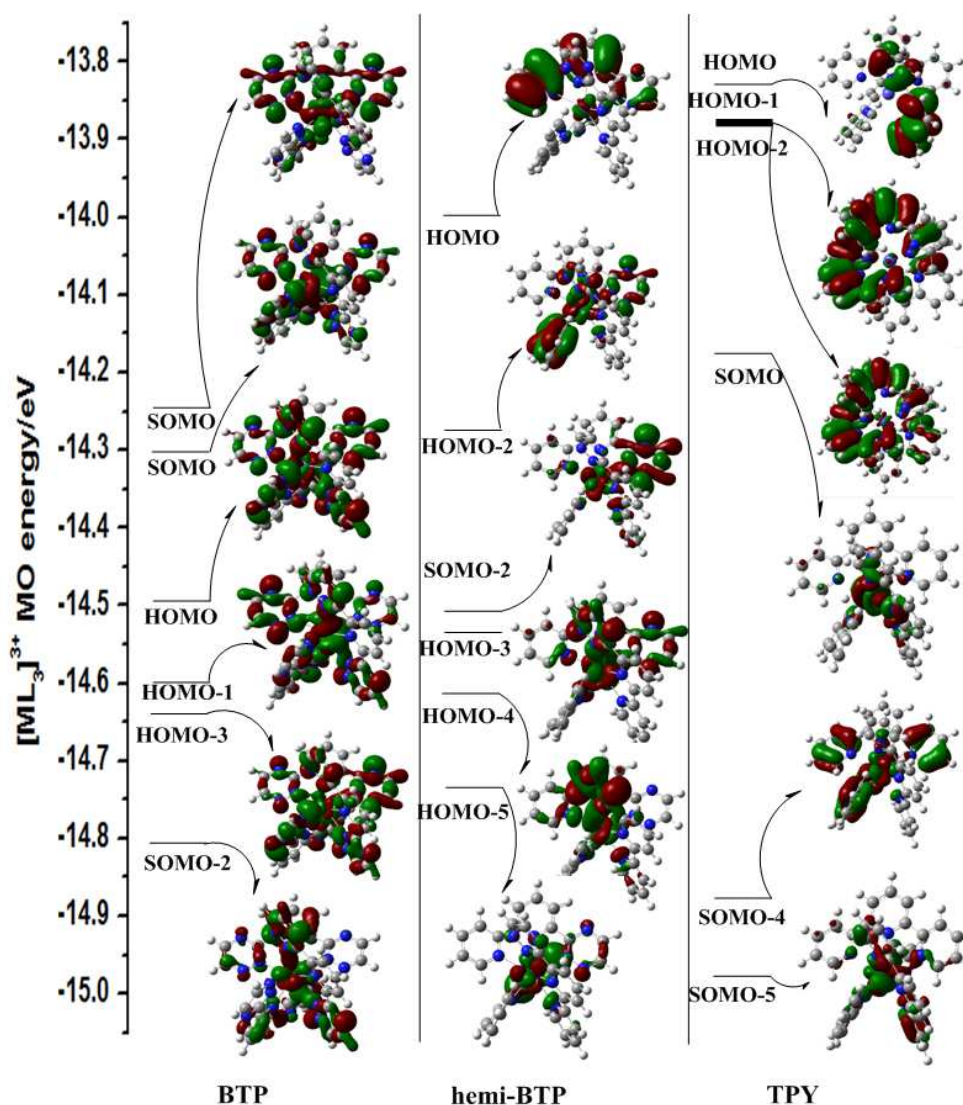
Figure 6. Representative α-Spin MOs of $[AmL_3]^{3+}$ in the gas phase. The corresponding contributions of metal atom are listed in Table 6.The isosurface value of MO is 0.02 au.

For hemi-BTP, the HOMO is mainly localized in the ligands. For the doubly occupied orbitals, the orbital overlap character is smaller than $[ML]^{3+}$, the metal-to-ligand back-donation mainly occurred involving the ligand σ orbital and the empty metal orbitals.

For the complex of L=TPY, the first three doubly occupied orbitals are mainly the ligand π orbitals, and there is no molecular orbital overlap between the metal orbitals and the ligand orbitals until SOMO-4, where small component of metal-to-ligand back-donation is observed involving the metal singly occupied $5f$ orbitals and the σ orbitals of the coordinated N atom.

Overall, the more stable the complexes, the less molecular orbital overlap between the σ ligand orbitals and the metal $5f$ orbitals. The frontier orbital analysis is consistent with the above-mentioned bond orders and NPA, and supports that the metal-ligand bond is predominantly ionic. Covalency is present through ligand-to-metal electron donation and slightly more pronounced for ligand BTP than for TPY.

3.6 The ligand reactions of Am(III) in the gas phase and aqueous solution

In aqueous solution, the spherical Am(III) ion favors a coordination number of 8 or 9 in its hydrated form.[48, 49] Previous B3LYP calculations[22] show that $[Am(H_2O)_9]^{3+}$ is more favorable than $[Am(H_2O)_8]^{3+}$ in the gas phase, while $[Am(H_2O)_8]^{3+}$ becomes slightly more stable when solvent effect is taken into account. It is possible for the two hydrated species to co-exist in aqueous solution in a thermodynamic equilibrium.[50, 51]

3.6.1. Ligand exchange between water and nitrate ion. In this work, $[Am(H_2O)_9]^{3+}$ was used to represent the hydrated species, and the coordinated water molecules may be replaced by the other ligands via ligand exchange reactions which can be either thermoneutral or exothermic. In the presence of NO_3^-, nitrated complexes in their hydration form may be produced with NO_3^- appearing as a bidentate ligand. In Table 7 the Gibbs free energy changes for the formation of nitrated complexes are collected, and the negative ΔG_s values for the reactions $[Am(H_2O)_9]^{3+} + nNO_3^- \rightarrow [Am(NO_3)_n(H_2O)_{9-n}]^{3-n}$ (n=1-4) suggest that these processes are favorable both in the gas phase and in aqueous solution.

Table 7. Gibbs Free Energy changes (kcal mol^{-1}) of the nitration reactions of $[Am(NO_3)_n(H_2O)_m]^{3-n}$ (m=3,5,7,9 and n=0-3) in the gas phase (ΔG_g) and aqueous solution (ΔG_s) at the B3LYP/BS1 level.

Complexation reactions	ΔG_g	ΔG_s
$[M(H_2O)_9]^{3+} + NO_3^- \rightarrow [M(NO_3)(H_2O)_7]^{2+} + 2H_2O$	-253.2	-24.6
$[M(NO_3)(H_2O)_7]^{2+} + NO_3^- \rightarrow [M(NO_3)_2(H_2O)_5]^+ + 2H_2O$	-180.6	-20.0
$[M(NO_3)_2(H_2O)_5]^+ + NO_3^- \rightarrow M(NO_3)_3(H_2O)_3 + 2H_2O$	-112.5	-15.6
$[M(NO_3)_3(H_2O)_3] + NO_3^- \rightarrow [M(NO_3)_4(H_2O)]^- + 2H_2O$	-42.0	-15.8
$[M(NO_3)_2(H_2O)_5]^+ + H_2O \rightarrow [M(NO_3)_2(H_2O)_6]^+$	-9.2	0.2
$[M(NO_3)_3(H_2O)_3] + H_2O \rightarrow [M(NO_3)_3(H_2O)_4]$	-4.8	3.3

As shown in Table 7, the nitration of hydrated Am(III) ion is thermodynamically favorable with Am coordinated to as many as four nitrate ions, reaching a C.N. of 9, and the nine

coordinated $[Am(NO_3)_4(H_2O)]^-$ complex may be formed in nitrate-rich acidic solution via further nitration of the neutral complex $Am(NO_3)_3(H_2O)_3$ with Gibbs free energy changes of $\Delta G_g = -42.0$ kcal mol^{-1} and $\Delta G_s = -15.8$ kcal mol^{-1}.

Retegan et al.[52] suggested a complexation process of $Am^{3+} + nH_2O + 3NO_3^- \rightarrow Am(NO_3)_3(H_2O)_n$ in acid solution, where $n = 4\text{-}6$. In our DFT calculations, three water molecules may coordinate to the metal center with a coordination number (CN.) of 9 at most, and the addition of one more water molecule to $Am(NO_3)_3(H_2O)_3$ to form another neutral complex $Am(NO_3)_3(H_2O)_4$ is only marginally exothermic in the gas phase ($\Delta G_g = -4.8$ kcal mol^{-1}) while endothermic in aqueous phase ($\Delta G_s = 3.3$ kcal mol^{-1}).

The formation of the complex $[Am(NO_3)_2(H_2O)_6]^+$ from $[Am(NO_3)_2(H_2O)_5]^+$ is thermodynamically favorable in the gas phase. In aqueous solution, it becomes marginally endothermic with $\Delta G_s = 0.2$ kcal mol^{-1} owing to the solvation effect, and an equilibrium may exist between these two species.

3.6.2. Ligand exchange between water and L. Earlier studies[52, 53] suggested the coordination of ligand to metal may follow the mechanism of $Am(NO_3)_3 + L \rightarrow AmL(NO_3)_3$. A later B3LYP study proposed to take into account water molecules in the first coordination shell of M^{3+}, i.e. $M(NO_3)_3(H_2O)_4 + L \rightarrow ML(NO_3)_3 + 4(H_2O)$ (M=Am or Eu; L=BTBPs).[22, 27]

It is conceivable that in aqueous phase, the large ionic radius of Am and its complex outer shell atomic orbitals make it highly probable to appear with high coordination numbers given sufficient space in its surrounding area. Here, the hydrated form of nitrated Am(III), $Am(NO_3)_3(H_2O)_3$, was used as the starting material to analyze the complexation mechanism of the tridentate N-donor ligands with Am(III). The calculations show that the complexation reactions

$$Am(NO_3)_3(H_2O)_3 + L \rightarrow AmL(NO_3)_3 + 3(H_2O) \text{ (L=BTP, hemi-BTP, TPY)} \quad (2)$$
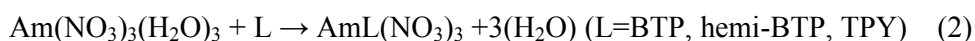
are all exothermic both in the gas phase and aqueous solution, and the Gibbs free energy change is more negative when the lateral 1,2,4-triazine is replaced by pyridine, i.e. in the order of BTP < hemi-BTP < TPY.

As the complexation reaction (2) is one of the possible channels of Am(III)/Eu(III) separation, and the thermodynamics is influenced by the type of the extractant and the stability of the complex $AmL(NO_3)_3$, here we calculated the changes of the Gibbs free energy of reaction (2) for a series of ligands, as shown in Figure 7. Based on our calculations, ligands baring

electron-donating group is thermodynamically more favourable to substitute for three water molecules to form the $AmL(NO_3)_3$ complexes. The ligands with MeOPh and $CyMe_4$ substituents exhibited equally strong binding ability with Am(III), which is consistent with previous work in which the ligand $CyMe_4$-BTBP[54] is shown to be the most suitable for An(III)/Ln(III) separations under reprocessing conditions.[55] Taking into account solvent effect favors the ligand exchange reactions, as shown in Figure 7.
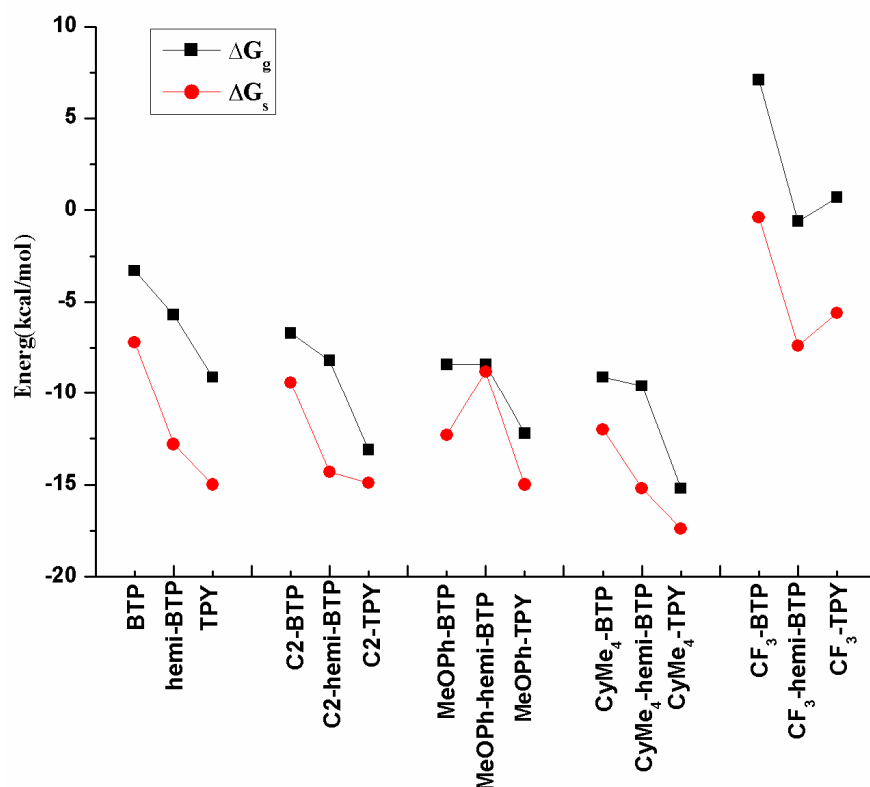
Figure 7. The Gibbs free energy changes (kcal mol^{-1}) for the ligand exchange reactions $Am(NO_3)_3(H_2O)_3 + L \rightarrow AmL(NO_3)_3 + 3(H_2O)$ (M=Am) in the gas phase and aqueous solution calculated at the B3LYP/BS2 level.

We also investigated the replacement of NO_3^- by L, i.e. $[Am(NO_3)_4(H_2O)]^- + L \rightarrow AmL(NO_3)_3 + H_2O + NO_3^-$, and found the process was strongly endothermic in both gas and aqueous phases. For example, the endothermicity is up to 40 kcal mol^{-1} for BTP in the gas phase, as tabulated in Table 8. For the hydration reaction $AmL(NO_3)_3 + H_2O \rightarrow AmL(NO_3)_3(H_2O)$, ΔG_g and ΔG_s are all positive, except for the case of L=BTP where $\Delta G_g = -2.3$ kcal mol^{-1}, which suggests that the coordination of Am(III) is saturate in $AmL(NO_3)_3$, and thermodynamically it is less likely to be hydrated further.

According to the above description, to form 1:2 complexes, the presence of at least six

water molecules in the complex is required to allow for a thermodynamically favorable ligand exchange reaction to happen. Here we considered two complexes $[Am(NO_3)(H_2O)_7]^{2+}$ and $[Am(NO_3)_2(H_2O)_6]^+$, and the Gibbs free energy changes to the reactions are tabulated in Table 8.

Table 8. Gibbs Free Energy changes (kcalmol^{-1}) of complexation reactions for the formation of 1:1, 1:2 and 1:3 complexes in the gas phase and aqueous solution at the B3LYP/BS1 level.

Complexation reactions	ΔG_g			ΔG_s		
	BTP	hemi-BTP	TPY	BTP	hemi-BTP	TPY
$M^{3+} + L \rightarrow [ML]^{3+}$	-387.9	-392.1	-399.5	-12.8	-21.1	-25.1
$M^{3+} + 2L \rightarrow [ML_2]^{3+}$	-556.2	-562.1	-571.7	-23.5	-31.3	-38.1
$M^{3+} + 3L \rightarrow [ML_3]^{3+}$	-631.1	-626.1	-629.6	-27.6	-28.6	-35.7
$[ML]^{3+} + L \rightarrow [ML_2]^{3+}$	-168.3	-170.0	-172.3	-10.7	-10.3	-12.9
$[ML_2]^{3+} + L \rightarrow [ML_3]^{3+}$	-74.9	-64.1	-57.9	-4.0	2.7	2.4
$[M(H_2O)_9]^{3+} + 3L \rightarrow [ML_3]^{3+} + 9H_2O$	-142.3	-137.3	-140.8	-29.2	-30.2	-37.2
$[M(H_2O)_9]^{3+} + L \rightarrow [ML(H_2O)_6]^{3+} + 3H_2O$	-65.4	-65.3	-63.3	-14.4	-15.3	-14.4
$[ML(H_2O)_6]^{3+} + L \rightarrow [ML_2(H_2O)_3]^{3+} + 3H_2O$	-45.1	-44.2	-43.8	-11.6	-14.1	-14.1
$[ML_2(H_2O)_3]^{3+} + L \rightarrow [ML_3]^{3+} + 3H_2O$	-31.8	-27.8	-33.7	-3.2	-0.8	-8.7
$[ML_2(NO_3)(H_2O)]^{2+} + NO_3^- \rightarrow [ML_2(NO_3)_2]^+ + H_2O$	-152.6	-155.3	-153.6	-15.2	-16.3	-13.8
$[ML_2]^{3+} + 2NO_3^- \rightarrow [ML_2(NO_3)_2]^+$	-401.2	-395.5	-389.0	-31.6	-27.6	-23.8
$M(NO_3)_3 + L \rightarrow ML(NO_3)_3$	-35.7	-38.2	-41.9	-5.7	-10.9	-13.8
$M(NO_3)_3(H_2O)_3 + L \rightarrow ML(NO_3)_3 + 3H_2O$	-1.6	-4.1	-7.8	-6.6	-11.8	-14.7
$ML(NO_3)_3 + H_2O \rightarrow ML(NO_3)_3(H_2O)$	-2.3	0.0	2.9	4.4	4.1	5.8
$[M(NO_3)(H_2O)_7]^{2+} + 2L \rightarrow [ML_2(NO_3)(H_2O)]^{2+} + 6H_2O$	-62.8	-60.3	-65.0	-16.9	-19.6	-25.1
$[M(NO_3)_2(H_2O)_6]^+ + 2L \rightarrow [ML_2(NO_3)_2]^+ + 6H_2O$	-25.5	-25.7	-28.8	-12.3	-16.1	-19.1
$[M(NO_3)_4(H_2O)]^- + L \rightarrow ML(NO_3)_3 + NO_3^- + H_2O$	40.3	37.8	34.1	9.2	4.0	1.1

The complexation reactions of $[Am(NO_3)(H_2O)_7]^{2+} + 2L \rightarrow [AmL_2(NO_3)(H_2O)]^{2+} + 6H_2O$ and $[Am(NO_3)_2(H_2O)_6]^+ + 2L \rightarrow [AmL_2(NO_3)_2]^+ + 6H_2O$ are exothermic in both phases. For the reaction $[AmL_2(NO_3)(H_2O)]^{2+} + NO_3^- \rightarrow [AmL_2(NO_3)_2]^+ + H_2O$, ΔG_g and ΔG_s are all much negative, which indicated the presence of a second NO_3^- in the 1:2 complexes$[AmL_2(NO_3)(H_2O)]^{2+}$, i.e. the formation of $[AmL_2(NO_3)_2]^+$, may bring further stabilization. This leads us to deduce that the most stable 1:2 complex of Am(III) with BTP, hemi-BTP and TPY is $[AmL_2(NO_3)_2]^+$, and the reaction

$$[Am(NO_3)_2(H_2O)_6]^+ + 2L \rightarrow [AmL_2(NO_3)_2]^+ + 6H_2O \quad (3)$$
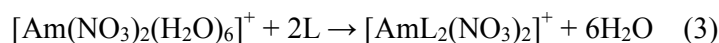
is probably the dominant path for the 1:2 complexation. For the reaction (3), the Gibbs free energy change increases in the order of BTP < hemi-BTP < TPY, and the solvent effects

26

enhance the difference of the Gibbs free energy change between them.

For the 1:3 complexes, nine water molecules were replaced to form $[AmL_3]^{3+}$. The Gibbs free energy changes are all much negative, indicating these ligand exchange reactions are strongly exothermic. Similar to the cases of 1:1 and 1:2 complexes, Am(III) displays stronger binding affinity to TPY than to the other two ligands. Considering a stepwise mechanism for the ligand exchange reactions towards the formation of AmL_3 from $Am(H_2O)_9$ in the absence of nitrate ions, i.e.

(a) $[Am(H_2O)_9]^{3+} + L \rightarrow [AmL(H_2O)_6]^{3+} + 3\ H_2O,$

(b) $[AmL(H_2O)_6]^{3+} + L \rightarrow [AmL_2(H_2O)_3]^{3+} + 3\ H_2O,$ and

(c) $[AmL_2(H_2O)_3]^{3+} + L \rightarrow [AmL_3]^{3+} + 3\ H_2O,$
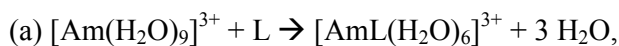
The Gibbs free energy changes of these reactions are all negative for the three ligands, suggesting the propensity for the formation of the 1:3 type complexes $[AmL_3]^{3+}$ in the absence of nitrate ion.

To explore the relationship between the stability of complexes and the complexation reactions including water molecules and nitrate ions, the binding free energies of the studied Am(III) complexes were calculated according to the equation below:

$$\Delta G = G\ ([AmL_n]^{3+}) - G\ (Am^{3+}) - n\ G(L)$$

where G is the Gibbs free energy. The results are tabulated in Table 8.

For the 1:1 and 1:2 complexes $[AmL]^{3+}$ and $[AmL_2]^{3+}$, the thermal stability increases in the order of BTP < hemi-BTP < TPY both in the gas phase and aqueous solution. For the 1:3 complex $[AmL_3]^{3+}$, in the gas phase the BTP complex is the most stable in view of energy while hemi-BTP complex is the most unstable. When solvent effect of water is taken into account, the TPY complex is preferable in view of binding energy.

According to our calculations, consider a stepwise pathway for the formation of $[AmL_3]^{3+}$, i.e. $[AmL]^{3+} \rightarrow [AmL_2]^{3+} \rightarrow [AmL_3]^{3+}$, TPY and hemi-BTP prefer to form 1:1 and 1:2 complexes while BTP the more hydrophobic 1:3 complexes both in the gas phase and aqueous solution, which is consistent with previous extraction experiments.[56]

To explore the M-L bonding nature of 1:1 to 1:3 metal-to-ligand complexes, the metal-ligand bond lengths and their Mayer bond order, the NPA charge of Am, and the 5f-orbital occupancy were also analyzed and presented in Table 9. It can be seen the natural

charges of Am^{3+}, and the Am-N bond orders as well, decrease significantly from 1:1 to 1:3 complexes independent of the presence of nitrate ions, indicating the enhanced donor-acceptor interaction in the more hydrophobic 1:3 complexes. For 1:1 and 1:2 type complexes, the Am-N bond distances of the TPY complexes are somewhat shorter than that of BTP complexes, suggesting a stonger Am-N bond interaction in the TPY complexes.

Table 9. Calculated Am-N and Am-O distances (d, in Å), the Mayer bond order (MBO), the NPA charge of Am^{3+} (q_M), and 5f orbital occupancy of 1:1 to 1:3 complexes in the gas phase.

L	d_{Am-L}				MBO				q_M	Occ.(5f)
	N_1	N_2	N_4	O	N_1	N_2	N_4	O		
$[AmL]^{3+}$										
BTP	2.58	2.32	-	-	0.41	0.48	-	-	2.230	6.35
hemi-BTP	2.49	2.31	2.37	-	0.48	0.49	0.57	-	2.270	6.29
TPY	2.44	2.42	-	-	0.47	0.50	-	-	2.174	6.44
$[AmL_2]^{3+}$										
BTP	2.58	2.47	-	-	0.34	0.33	-	-	1.873	6.15
hemi-BTP	2.55	2.46	2.49	-	0.36	0.32	0.40	-	1.866	6.14
TPY	2.52	2.48	-	-	0.37	0.40	-	-	1.860	6.14
$[AmL_3]^{3+}$										
BTP	2.64	2.63	-	-	0.25	0.23	-	-	1.431	6.08
hemi-BTP	2.66	2.64	2.66	-	0.26	0.23	0.28	-	1.461	6.08
TPY	2.66	2.67	-	-	0.26	0.28	-	-	1.494	6.08
$[AmL(NO_3)_3]$										
BTP	2.72	2.65	-	2.47	0.18	0.17	-	0.36	1.434	6.16
hemi-BTP	2.70	2.62	2.65	2.48	0.19	0.18	0.23	0.34	1.418	6.15
TPY	2.65	2.64	-	2.48	0.21	0.23	-	0.34	1.408	6.15
$[AmL_2(NO_3)_2]^+$										
BTP	2.69	2.66	-	2.51	0.20	0.18	-	0.34	1.265	6.14
hemi-BTP	2.69	2.67	2.68	2.51	0.21	0.18	0.24	0.33	1.269	6.13
TPY	2.67	2.68	-	2.52	0.22	0.23	-	0.33	1.256	6.13
$[AmL(H_2O)_6]^{3+}$										
BTP	2.66	2.64	-	2.54	0.27	0.26	-	0.30	1.544	6.10
hemi-BTP	2.59	2.63	2.55	2.58	0.31	0.27	0.35	0.28	1.537	6.10
TPY	2.58	2.57	-	2.59	0.32	0.34	-	0.27	1.557	6.08
$[AmL_2(H_2O)_3]^{3+}$										
BTP	2.65	2.64	-	2.53	0.27	0.23	-	0.32	1.489	6.10
hemi-BTP	2.65	2.67	2.65	2.53	0.28	0.23	0.28	0.33	1.489	6.10
TPY	2.63	2.62	-	2.63	0.30	0.30	-	0.25	1.501	6.11

The small bond order values of Am-L bonds suggest that the ionic interaction may be predominant for these complexes. The natural charges of Am^{3+} indicated larger shifts of

electron density from TPY than from BTP to Am^{3+}, and the electrostatic interactions may largely govern both TPY and BTP complexes, as Retegan et al. proposed.[57] For the 1:3 complexes $[AmL_3]^{3+}$, the L-to-M electron transfer decreases along BTP > hemi-BTP > TPY, which shows stronger ionic interactions between Am(III) and BTP results in the formation of the more stable 1:3 complexes. For all hemi-BTP complexes in Table 9, the Mayer bond order of M-N$_4$ is larger than that of M-N$_2$ regardless of M-N bond lengths, indicating the lateral pyridine rings interacts with Am^{3+} with more covalency feature than the lateral triazine rings.

4. Conclusions

By means of DFT calculations, we investigated the possible complexation modes of Am(III) with three tridentate N-donor ligands, i.e. BTP, hemi-BTP and TPY in various stoichiometric ratios of Am:L = 1:1, 1:2 and 1:3. The effect of R-substituents on the stability of complexes was studied by taking the 1:1 complexes $[AmL]^{3+}$ and $AmL(NO_3)_3$ as examples. The changes of the Gibbs free energy for the possible reactions were calculated in both gas phase and aqueous solution to study the complexation mechanism and binding mode of tridentate N-donor ligands with Am(III), and conclusions below may be drawn:

(1) Based on the Gibbs free energy change, for 1:1 type complexes, the reaction of $Am(NO_3)_3(H_2O)_3 + L \rightarrow AmL(NO_3)_3 + 3H_2O$ is probably one of the dominant reactions in Am(III) extraction. The donor-acceptor interaction in 1:2 complexes is enhanced compared to that in 1:1 complexes. The reaction of $[Am(NO_3)_2(H_2O)_6]^+ + 2L \rightarrow [AmL_2(NO_3)_2]^+ + 6H_2O$ is more likely one of the complexation reactions for 1:2 type complexes. The formation of 1:3 type complexes were also considered via reactions of $[Am(H_2O)_9]^{3+} \rightarrow [AmL_3]^{3+}$ and $[AmL_2]^{3+} \rightarrow [AmL_3]^{3+}$. In view of the Gibbs free energy change of the complexation reactions, hemi-BTP and TPY prefer to form 1:2 complexes, and BTP prefers to form 1:3 complexes. In addition, the TPY binds stronger with Am(III) than hemi-BTP does, and BTP complexes is the most unstable.

(2) For the complexes $[AmL]^{3+}$ and $AmL(NO_3)_3$, the comparison of substitution effect indicated that Ethyl, MeOPh as well as CyMe$_4$ groups can strengthen the binding stabilities of the R-BTPs, R-hemi-BTPs and R-TPYs complexes, indicating the beneficial effect of substituents with strong electron-donating ability. On the contrary, the electron-withdrawing group CF$_3$ decreases the binding strength of the BTPs complexes greatly.

(3) The analysis of NPA charges shows that the ligand-to-metal charge transfer is much higher in the complexes $[AmL]^{3+}$ with more negative binding energy. Meanwhile, Mayer bond order of the Am-N bond is lower than that of the less stable complexes. This suggests that the interaction between Am^{3+} and the ligand has strong ionic feature, which is confirmed by the QTAIM topological analysis. According to Mulliken population analysis on the frontier molecular orbital composition of $[AmL]^{3+}$, the partially occupied 5f orbitals do not contribute to the frontier occupation orbitals, and only a few inner MOs show a mixing between the ligand and the metal orbitals. The metal-to-ligand back-donation is much stronger than ligand-to-metal donation among three ligands, and it takes place mainly involving a singly occupied 5f orbital and ligand orbitals. For the $[AmL_3]^{3+}$ complexes of BTP, in contrast, the orbital overlap between the orbitals of ligand and 5f metal orbitals were shown significantly in occupied frontier orbitals.

(4) The comparison of the conformational transitions of the three types of ligands shows that in neutral or acidic solution, only BTP may realize facile transition to its *cis-cis* or *cis-trans* form which are favorable in complexation with Am(III), while hemi-BTP and TPY face sizeable energy demand to their tridentate forms, i.e. the *cis-cis* or *cis-trans* form of hemi-BTP and the *cis-cis* form of TPY. Meanwhile, TPY and hemi-BTP were also observed to be easier to be protonated than BTP thermodynamically, which brings adverse effect in their complexation with Am(III) in acidic media as deprotonation is required. The conformational preference of the three types of ligands, together with their different propensity to be protonated, constitutes an important force that determines their distinct performance in the extraction of Am(III).

Notes and references

1.   L. Cecille, M. Casarci and L. Pietrelli, *New Separation Chemistry Techniques for Radioactive W aste and*

other Specific Applications, Commission of the European Communities, Elsevier Applied Science, London, New York, , 1991.

2.   J. N. Mathur, M. S. Murali and K. L. Nash, *Solv. Extr. Ion. Exch.*, 2001, **19**, 357-390.

3.   C. M adic, M. Lecomte, P. Baron and B. Boullis, *C. R. Phys.* , 2002, **3**, 797-811.

4.   K. L. Nash, *Solv. Extr. Ion Exch.*, 1993, **11**, 729-768.

5.   H. H. Dam, D. N. Reinhoudt and W. Verboom, *Chem. Soc. Rev.* , 2007, **36**, 367-377.

6.   Z. Kolarik, U. Müllich and F. Gassner, *Solv. Extr. Ion Exch.*, 1999, **17**, 23-32.

7.   Z. Kolarik, U. Müllich and F. Gassner, 1999, **17**, 1155-1170.

8.   M. J. Hudson, M. G. B. Drew, M. R. St. J. Foreman, C. Hill, N. Huet, C. Madic and T. G. A. Youngs, *Dalton Trans.*, 2003, 1675-1685.

9.   P. Y. Cordier, P. B. C. Hill, C. Madic, M. J. Hudson and J.-O. Liljenzin, *J. Alloys Compd.* , 1998, **271**, 738-741.

10.   I. Hagström, L. Spjuth, Å. Enarsson, J.-O. Liljenzin, M. Skalberg, M. J. Hudson, P. B. Iveson, C. Madic, P. Y. Cordier, C. Hill and N. Francois, *Solv. Extr. Ion Exch.*, 1999, **17**, 221-242.

11.   M. G. B. Drew, P. B. Iveson, M. J. Hudson, J.-O. Liljenzin, L. Spjuth, P.-Y. Cordier, Å. Enarsson, C. Hill and C. Madic, *J. Chem. Soc., Dalton Trans.* , 2000, **5**, 821-830.

12.   F. W. Lewis, L. M. Harwood, M. J. Hudson, M. G. B. Drew, M. Sypula, G. Modolo, D. Whittaker, C. A. Sharrad, V. Videva, V. Hubscher-Bruder and F. Arnaud-Neu, *Dalton Trans.*, 2012, **41**, 9209-9219.

13.   M. J. Hudson, M. R. S. J. Foreman, C. Hill, N. Huet and C. Madic, *Solv. Extr. Ion Exch.*, 2003, **21**, 637-652.

14.   G. Ionova, C. Rabbe, R. Guillaumont, S. Ionov, C. Madic, J. C. Krupa and D. Guillaneux, *New J. Chem.* , 2002, **26**, 234-242.

15.   D. Guillaumont, *J. Phys. Chem. A* 2004, **108**, 6893-6900.

16.   R. G. Parr and W. Yang, *Density-Functional Theory of Atoms and Molecules*, Oxford University Press, Oxford, U.K., 1989.

17.   L. Petit, C. Adamo and P. Maldivi, *Inorg. Chem*, 2006, **45**, 8517-8522.

18.   A. Klamt and G. Schüürmann, *J. Chem. Soc., Perkin Trans.*, 1993, **2**, 799-805.

19.   A. Klamt, *J. Phys. Chem.* , 1995, **99**, 2224-2235.

20.   A. Klamt and V. Jones, *J. Chem. Phys.* , 1996, **105**, 9972-9981.

21.   M. Miguirditchian, D. Guillaneux, D. Guillaumont, P. Moisy, C. Madic, M. P. Jensen and K. L. Nash, *Inorg. Chem.* , 2005, **44**, 1404-1412.

22.   J.-H. Lan, W.-Q. Shi, L.-Y. Yuan, Y.-X. Feng, Y.-L. Zhao and Z.-F. Chai, *J. Phys. Chem. A* 2012, **116**, 504-511.

23.   A. Bhattacharyya, E. Kim, P. F. Weck, P. M. Forster and K. R. Czerwinski, *Inorg. Chem.*, 2013, **52**, 761-776.

24.   G. Benay, R. Schurhammer and G. Wipff, *Phys. Chem. Chem. Phys.*, 2011, **13**, 2922-2934.

25.   G. Benay, R. Schurhammer, J. Desaphy and G. Wipff, *New J. Chem.*, 2011, **35**, 184-189.

26.   J. Narbutt and W. P. Oziminski, *Dalton Trans.*, 2012, **41**, 14416-14424.

27.   J.-H. Lan, W.-Q. Shi, L.-Y. Yuan, Y.-L. Zhao, J. Li and Z.-F. Chai, *Inorg. Chem.*, 2011, **50**, 9230-9237.

28.   C. Lee, W. Yang and R. G. Parr, *Phys. Rev. B*, 1988, **37**, 785-789.

29.   A. D. Becke, *J. Chem. Phys.*, 1993, **98**, 5648-5652.

30.   P. J. Stephens, F. J. Devlin, C. F. Chabalowski and M. J. Frisch, *J. Phys. Chem.*, 1994, **98**, 11623-11627.

31.   R. C. Gaussian 09, M. J. Frisch, G. W. Trucks, H. B. Schlegel, G. E. Scuseria, M. A. Robb, J. R. Cheeseman, G. Scalmani, V. Barone, B. Mennucci, G. A. Petersson, H. Nakatsuji, M. Caricato, X. Li, H. P. Hratchian, A. F. Izmaylov, J. Bloino, G. Zheng, J. L. Sonnenberg, M. Hada,   M. Ehara, K. Toyota, R.

Fukuda, J. Hasegawa, M. Ishida, T. Nakajima, Y. Honda, O. Kitao, H. Nakai, T. Vreven, J. A. Montgomery, Jr., J. E. Peralta, F. Ogliaro, M. Bearpark, J. J. Heyd, E. Brothers, K. N. Kudin, V. N. Staroverov, T. Keith, R. Kobayashi, J. Normand, K. Raghavachari, A. Rendell, J. C. Burant, S. S. Iyengar, J. Tomasi, M. Cossi, N. Rega, J. M. Millam, M. Klene, J. E. Knox, J. B. Cross, V. Bakken, C. Adamo, J. Jaramillo, R. Gomperts, R. E. Stratmann, O. Yazyev, A. J. Austin, R. Cammi, C. Pomelli, J. W. Ochterski, R. L. Martin, K. Morokuma, V. G. Zakrzewski, G. A. Voth, P. Salvador, J. J. Dannenberg, S. Dapprich, A. D. Daniels, O. Farkas, J. B. Foresman, J. V. Ortiz, J. Cioslowski, and D. J. Fox, Gaussian, Inc., Wallingford CT, 2010.

32.   W. Kuechle, M. Dolg, H. Stoll and H. Preuss, *J. Chem. Phys.* , 1994, **100**, 7535-7542.

33.   X. Cao, M. Dolg and H. Stoll, *J. Chem. Phys.*, 2003, **118**, 487-496.

34.   X. Cao and M. Dolg, *J. Molec. Struct. (Theochem)* 2004, **673**, 203-209.

35.   P. C. Hariharan and J. A. Pople, *Theoret. Chimica Acta* 1973, **28**, 213-222.

36.   R. Krishnan, J. S. Binkley, R. Seeger and J. A. Pople, *J. Chem. Phys.*, 1980, **72**, 650-654.

37.   J. Tomasi, B. Mennucci and R. Cammi, *Chem. Rev.*, 2005, **105**, 2999-3093.

38.   R. F. W. Bader, *Atoms in Molecules. A Quantum Theory*, Clarendon Press, Oxford, U.K., 1994.

39.   P. Popelier, *Atoms in Molecules. An Introduction*, Prentice Hall, Harlow, 2000.

40.   T. Lu and F. Chen, *J. Chem. Chem.*, 2012, **33**, 580-592.

41.   M. J. Hudson, C. E. Boucher, D. Braekers, J. F. Desreux, M. G. B. Drew, M. R. St J. Foreman, L. M. Harwood, C. Hill, C. Madic, F. Marken and T. G. A. Youngs, *New J. Chem.*, 2006, **30**, 1171-1183.

42.   V. A. Palm, *Tables of Rate and Equilibrium Constants of Heterolytic Organic Reactions*, Academy of Science of the USSR, Moscow,, 1976.

43.   C.-C.Wang, T.-H.Tang and Y. Wang, *J. Phys. Chem. A*, 2000, **104**, 9566-9572.

44.   R. W. B. Bader, *Atoms in Molecules: A Quantum Theory; *, Oxford University Press, Oxford, U.K., 1990.

45.   H. L. Schmider and A. D. Becke, *J. Mol. Struct. (Theochem)* 2000, **527**, 51-61.

46.   H. L Schmider and A. D. Becke, *J. Chem. Phys.*, 2002, **116**, 3184-3193.

47.   R. G. Pearson, *Proc. Natl. Acad. Sci. U. S. A.*, 1986, **83**, 8440-8441.

48.   J. Wiebke, A. Moritz, X. Cao and M. Dolg, *Phys. Chem. Chem. Phys.*, 2007, **9**, 459-465.

49.   J. Ciupka, X. Cao-Dolg, J. Wiebke and M. Dolg, *Phys. Chem. Chem. Phys.*, 2010, **12**, 13215-13223.

50.   L. Helm and A. E. Merbach, *Coord. Chem. Rev.*, 1999, **187**, 151-181.

51.   L. Helm and A. E. Merbach, *Chem. Rev.*, 2005, **105**, 1923-1959.

52.   T. Retegan, C. Ekberg, I. Dubois, A. Fermvik, G. Skarnemark and T. J. Wass, *Solv. Extr. Ion Exch.* , 2007, **25**, 417-431.

53.   M. Nilsson, S. Andersson, F. Drouet, C. Ekberg, M. Foreman, M. Hudson, J. O. Liljenzin, D. Magnusson and G. Skarnemark, *Solv. Extr. Ion Exch.*, 2006, **24**, 299-318.

54.   A. Geist, C. Hill, G. Modolo, M. W. M. R. St. J. Foreman, K. Gompper, M. J. Hudson and C. Madic, *Solv. Extr. Ion Exch.*, 2006, **24**, 463-483.

55.   D. Magnusson, B. Christiansen, M. R. S. Foreman, J.-P. G. A. Geist, R. Malmbeck, G. Modolo, D. Serrano-Purroy and C. Sorel, *Solv. Extr. Ion Exch.*, 2009, **27**, 97-106.

56.   E. C. Constable, S. M. Elder and D. A. Tocher, *Polyhedron* 1992, **11**, 2599-2604.

57.   T. Retegan, L. Berthon, C. Ekberg, A. Fermvik, G. Skarnemark and N. Zorz, *Solv. Extr. Ion Exch.*, 2009, **27**, 663-682.

TOC: BTP differs from hemi-BTP and TPY in their conformational preference, which may contribute to its higher efficiency to extract Am(III).

AmL(NO₃)₃   [AmL₂(NO₃)₂]⁺   [AmL₃]³⁺(L=BTP)